

Design and Fabrication of Enhanced Anti-Reflective Properties using Pyramid/Nanowire Texturization of the Silicon Surface

Najmeh Kavooosi¹, Moosareza Safinejad¹, Mahdiyeh Mehran^{1,*}, Arash Mokhtari², and Fatemeh Fouladi Mahani²

¹RF MEMS and Bio-Nano Electronics (MBNE) Lab, Department of Electrical Engineering, Shahid Bahonar University of Kerman, Kerman, Iran

²Optical and RF Communication Systems (ORCS) Lab, Department of Electrical Engineering, Shahid Bahonar University of Kerman, Kerman 7616914111, Iran

(*) Corresponding author: m.mehran@uk.ac.ir

(Received: 30 June 2020 and Accepted: 29 August 2021)

Abstract

This paper proposes an enhanced anti-reflective surface by applying pyramid/nanowire textures to the silicon wafer. Before texturization, for the first time, we applied a pre-treatment process to the Si wafers using silver assisted chemical etching (MACE) process, which makes the silicon wafer porous. This porosity affects formation of the later synthesized micro pyramids with more uniformity in shape and distribution. For pyramid formation, the etching process of the p-type (100) silicon wafers in the KOH solution with different concentrations of 3, 5, and 7 wt.% along with the isopropyl alcohol is accomplished and surveyed. Micro pyramids are realized with different sizes based on the KOH concentration. In continue, the MACE process with Ag is applied to the pre-formed pyramids to realize the Si nanowires. Therefore, composite texturization of the silicon substrate is achieved. These combined nanowire/pyramid structures significantly reduce the light reflection of the silicon substrate. The acquired reflection factors are less than 3% (<3%). X-ray diffraction (XRD) is utilized to study the synthesized structures' crystalline characteristics which reveals the Si-cubic structure. Moreover, Raman spectroscopy results of the samples are also proposed.

Keywords: Anti-reflective surface, Pyramid/nanowire structures, Silicon solar cells, Surface texturization, MACE.

1. INTRODUCTION

Nowadays, solar cells play an important role among various energy resources providing powerful incentives for the development of renewable energy technologies. Silicon is a suitable material for employment in the photovoltaic industry [1, 2]. Silicon is an abundant material in nature, mostly used in the microelectronics industry thanks to its different advantages such as low cost, non-toxicity, good durability, and compatibility with the complementary metal-oxide-semiconductor (CMOS) technology [3, 4]. Due to the high reflectivity of the silicon surface, many studies and efforts have been performed to reduce the surface reflection of the silicon solar cells e.g. employing anti-

reflection coatings or textured surfaces [5]. TiO_x, SiO_x, and ZnO have been used to realize anti-reflective coatings in other areas such as displays, optical lenses, military and defense applications [6]. These coatings, however, suffer from instability, adhesion, and thermal imbalance [7]. The main techniques for texturization of the silicon substrate are wet and dry etching methods [8]. Laser structuring [9-11], plasma treatment [12, 13], electrochemical etching [14, 15], and reactive ion etching [16, 17] are some of the dry etching methods which need expensive and complex equipment [18]. Nowadays wet chemical etching methods for the fabrication of micro and nanostructures

have been quickly considered by researchers taking advantage of the simplicity, low cost, controllability of etching parameters, uniformity of the formed structures, applicability in the industry, and suitability of fabrication-specific structures [1,19, 20]. One of these methods is metal-assisted chemical etching (MACE), which has been performed by the solution of HF, H₂O₂, and metal catalysts such as Au, Cu, and especially Ag [7, 21-23]. Employing this process, different silicon nanostructures such as nanowire, nanohole, nanocone, nanopillar, as well as microstructures such as pyramids and inverted pyramids can be achieved [24-27]. Anisotropic etching of the silicon in the alkaline solutions with KOH, NaOH, and TMAH leads to the formation of pyramidal structures on its surface [23]. Texturization of the silicon substrate has been utilized to reduce surface reflection [28, 29]. Recently, a combination of the micro and nanostructures such as pyramids and nanowires [22], pyramids and nanoholes [30], inverted pyramids and nanowires [31], and inverted pyramids and nanoholes [32] have been employed which tends to the reduction in the reflection and the improvement of the incident light absorption. However, by controlling the fabrication process, reflection in the visible spectrum can be minimized [33].

In this work, double texturization of the silicon substrate in the form of nanowires on the micro pyramids is performed to achieve enhanced anti-reflective properties. Before the formation of the micro pyramids, for the first time, we pre-treatment Si wafers using the MACE process with Ag, which makes the silicon wafer porous. This porosity tends to the regular formation of the following synthesized micro pyramids. Then we investigate the effect of different KOH solution concentrations on the formation of micro pyramids. Consequently, silicon nanowires are formed on the bare and micro pyramids using the MACE process. The reflection behaviour of the bare silicon, differently formed micro-

pyramids, nanowires and double structures (micro pyramids/nanowires) are then surveyed. Synthesized silicon double structures in this paper show lower reflection compared to the previous works [7, 27, 33-36]. This paper is structured as the following: in the experimental section, the synthesis methods for the formation of micro/nanostructures are discussed. In the result and discussion section, reflection characteristics of the samples besides their XRD and Raman spectroscopy results are presented. This paper is terminated in the conclusion.

2. EXPERIMENTAL

A schematic of the proposed pyramid/nanowire textured silicon substrate is demonstrated in Fig. 1. For this study, p-type 1-5 Ω -cm (100) silicon wafers were employed. At first, wafers were immersed in the acetone bath for 10 minutes, washed with deionized (DI) water, and blown-dried. After that, they were cleaned using RCA#1 solution (NH₄OH: H₂O₂: H₂O, 1:1:5) for 10 minutes at 80 °C and immersed in the 38% hydrofluoric acid solution at room temperature for 10 seconds for removal of the native oxide. Subsequently, samples were immersed in the piranha solution (H₂SO₄: H₂O₂, 3: 1) at 80 °C for 10 minutes for the formation of a uniform oxide layer over the entire surface. This oxide helps uniformly distribution of the silver ions on the sample surface in the next step.

In this work, for the first time, silicon wafers were pre-treated using silver-assisted MACE process. This process makes silicon wafers porous and improves formation of the later micro pyramids. MACE is a two-step process. In the first step, silver ions were loaded to the silicon samples and in the second step; they were immersed in a solution of silver nitrate and hydrofluoric acid at room temperature. In this research, to realize deposition of the silver ions on the silicon samples, they were dipped in a solution of 4.8 M hydrofluoric acid (HF) and 0.02 M silver nitrate

(AgNO₃) for 10 seconds at the room temperature.

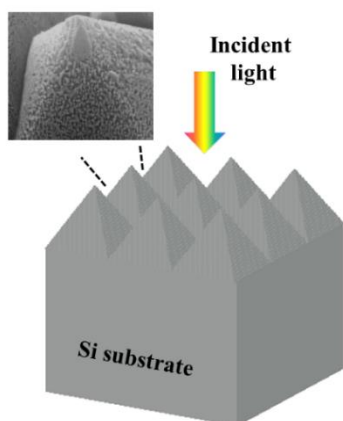


Figure 1. Schematic of the proposed pyramid/nanowire textured silicon wafer.

Then, they were washed with DI water and blown-dried. Afterwards, samples were transferred to a solution of 69% nitric acid for 5 minutes to remove the silver particles, then washed and blown-dried. This pre-treatment process improves the formation of the micro pyramids in the next step. In continue, for realization of the pyramid structures, three KOH solutions with different concentrations of 3 wt.%, 5 wt.% and 7 wt.% with IPA (5%) were prepared and samples were immersed in these solutions at 80 °C for 60 minutes.

In the following, the MACE process was employed again for engraving silicon nanowires on the bare and textured silicon substrates. To this end, silver ions were loaded on the samples in a 0.02 M silver nitrate and 4.8 M hydrofluoric acid solution for 10 seconds. Then, samples were washed immediately with the DI water, dried, and immersed in 69% nitric acid for 5 minutes for silver ions removal from the surface, so a porous surface remained. Afterwards, the samples were immersed in a solution of 0.02 M silver nitrate and 5 M hydrofluoric acid for 5 minutes at room temperature. After nanowires' formation, samples were washed in DI water, blown-dried, and immersed in the 69% nitric acid solution for removing silver ions residual between

nanowires. A schematic of the sequential steps depicting SiNWs fabrication on the micro-textured Si via MACE process in the AgNO₃ and HF solution is shown in Fig. 2. Morphology of the structures has been characterized by the field emission scanning electron microscope (FE-SEM). Furthermore, XRD results for surveying the crystalline characteristics of the synthesized structures are presented. Light reflection of the surface was measured by the ultraviolet-visible spectrophotometer with the wavelength range of 300-1000 nm. Moreover, Raman spectroscopy results are also proposed.

3. RESULTS AND DISCUSSION

Fig. 3 shows the pre-treatment effect on the silicon wafer using the MACE process with Ag. Fig. 3 (a) shows FE-SEM image of the bare silicon after cleaning, while Fig. 3 (b), illustrates loaded Ag nanoparticles on the silicon wafer during the MACE process. Porous silicon substrate after the MACE process is shown in Fig. 3 (c).

It is believed that the Si/AgNO₃/HF system in the MACE process is composed of a redox reaction: Ag⁺ ions are reduced in the cathodic reduction and in the anodic oxidation, dissolution of silicon which is locally beneath the Ag is occurred. Ag⁺ ions near the silicon surface, capture electrons from the valance band of Si and are deposited as the Ag nano-scale nuclei. These metallic Ag nuclei strongly attract electrons from Si and become negatively charged as they are more electronegative than Si. These Ag nuclei help the subsequent reduction of Ag ions, and facilitate Si oxidation so SiO₂ is produced underneath these Ag nanoparticles. In the following, shallow pits would form beneath the Ag nanoparticles, due to the etching of SiO₂ by the HF solution [37].

In the next step, employing anisotropic etching of crystalline silicon in the KOH solution, whole of the wafer surface was covered with the pyramidal structures.

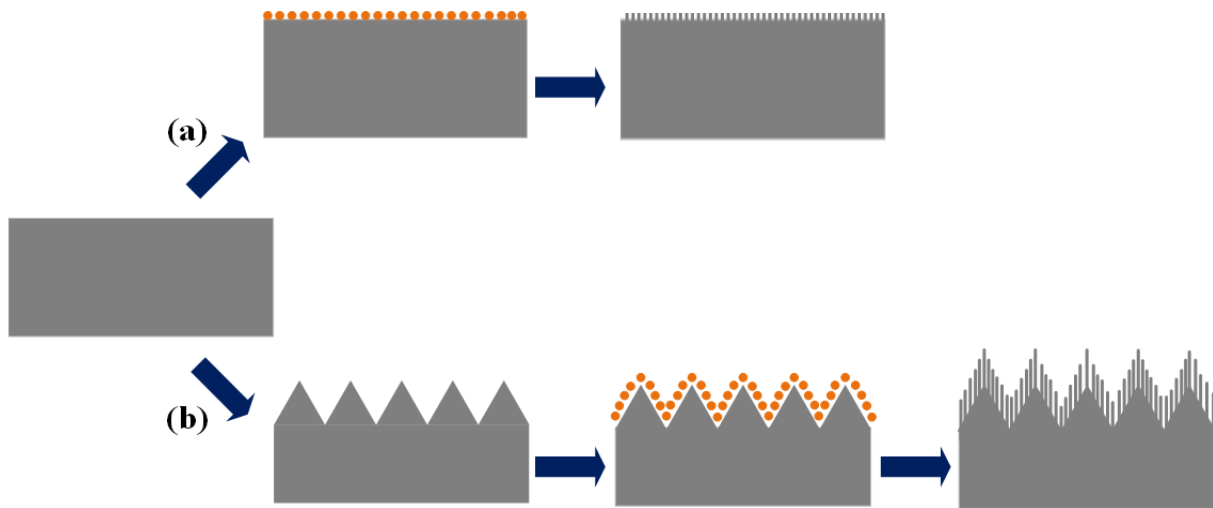


Figure 2. Schematic of the composite micro/nano texturization of the silicon substrate. Formation of (a) nanowires on the Si substrate using MACE process in the AgNO_3 and HF solution, (b) micro pyramids besides nanowires on the silicon substrate using conventional KOH etching of the Si besides MACE process.

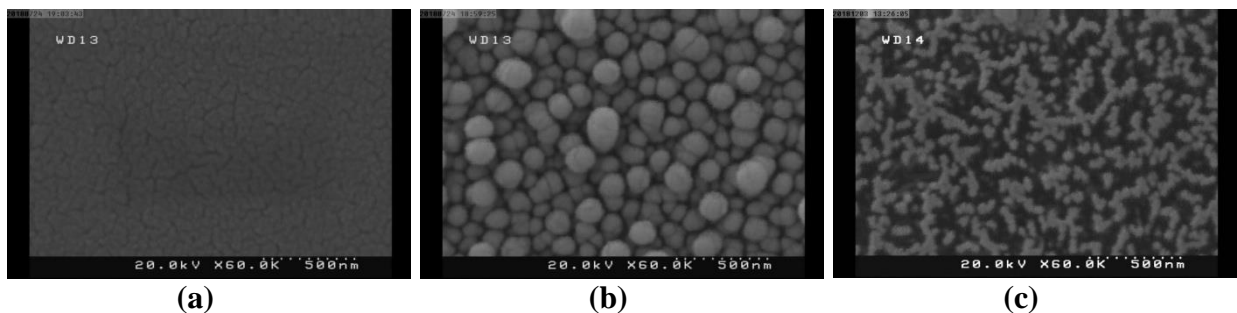


Figure 3. Effect of the pre-treatment of silicon wafer using MACE process with Ag, FE-SEM image of the, (a) bare silicon after cleaning, (b) loaded Ag nanoparticles on the silicon wafer and (c) the porous silicon substrate after MACE process.

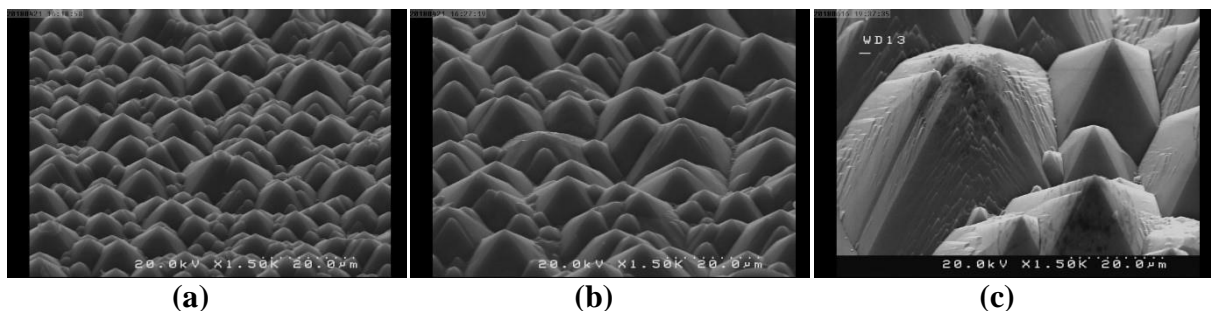


Figure 4. FE-SEM images of the synthesized pyramidal structures on the crystalline silicon wafers in the KOH solution with concentrations of (a) 3 wt.%, (b) 5 wt.%, and (c) 7 wt.%, for 60 minutes at 80°C .

Morphology of the formed pyramids on the silicon surface in different concentrations of the KOH solution was investigated.

Fig. 4 shows FE-SEM images of the synthesized pyramids in different KOH concentrations of 3 wt.%, 5 wt.%, and 7 wt.%. As it is obvious in these images, size

and distribution of the pyramids are directly proportional to the concentration of KOH solution. As the KOH concentration increases, bigger pyramids with more regular distribution are realized. The average size of 31.5, 52.8, and 120.7 μm has been achieved respectively for the formed pyramids in the KOH solutions with 3%, 5%, and 7% concentrations. Additionally, the average reflection of 9.81%, 11.002%, and 11.07%, respectively, in the range of 300-1000 nm, has been obtained from the surface of these pyramids. The bare silicon exhibits high average reflectance values exceeding 36.8%, whereas reflection from the textured Si decreases significantly to lower than 36.8%. This can be attributed to the fact that pyramid arrays give a second chance to the reflected light to be absorbed by the silicon substrate as the mirror behavior of the surface is reduced.

Fig. 5 shows the reflection profiles as a function of wavelength for the proposed structures and bare silicon wafer. As seen, the pyramidal structures reduce the light reflection and increase its absorption on the silicon wafer. As depicted before, pyramids which are formed in the 3 wt.% KOH solution show lower reflection than the other structures. The smaller size of pyramids, which are uniformly synthesized on the surface in this solution, results in a greater reduction in the reflection and increases absorption of the incident light.

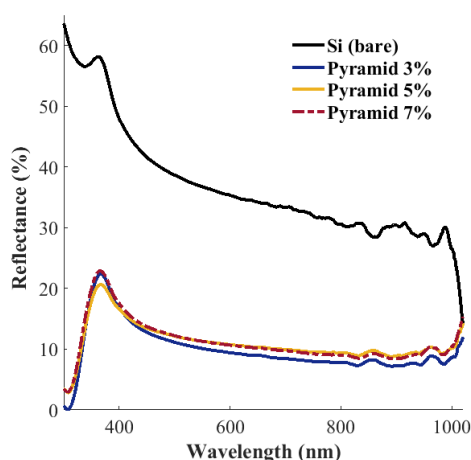


Figure 5. Reflectance spectra of the bare and pyramidal textured Si wafers in the

KOH solutions with concentrations of 3 wt.%, 5 wt.%, and 7 wt.%.

FE-SEM images of the Si nanowires and pyramid/nanowire double textured are shown in Fig. 6-a and 6-b, respectively. As it is obvious in these figures, the silicon surface has been modified with the micro and nanostructures. A combination of alkaline etching for the formation of pyramids and subsequent silver-assisted chemical etching has been employed for the formation of nanowires on the pyramids [35]. As said before, pyramids have been synthesized in different KOH solution concentrations.

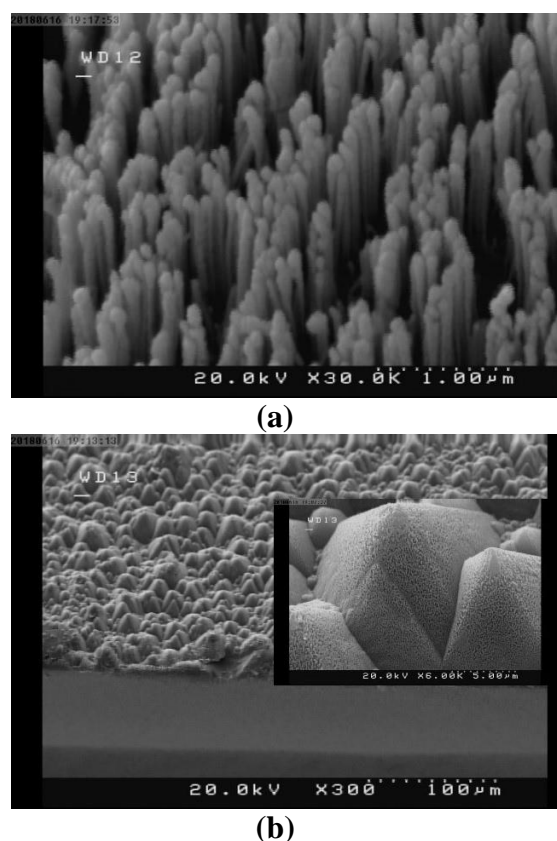


Figure 6. FE-SEM images of, (a) synthesized silicon nanowires with the MACE process and (b) composite pyramid/nanowire structure (pyramids are formed in the 3 wt.% of KOH solution).

Fig. 7 shows the reflection profiles of the polished silicon, nanowires on the silicon surface, and the pyramid/nanowire composite structure.

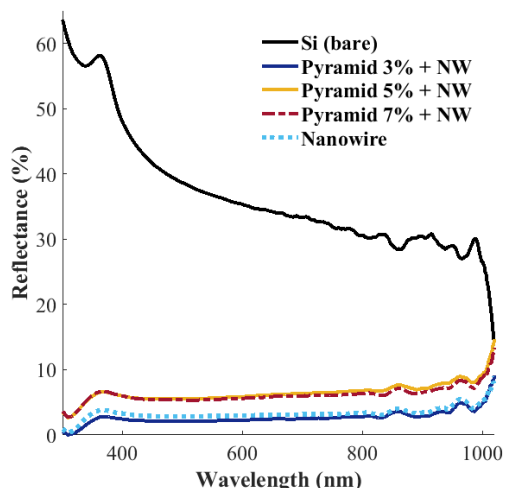


Figure 7. Reflectance spectra of the silicon wafer with different morphologies (bare, nanowire, pyramid 3 wt.%+NW, pyramid 5 wt.%+NW, and pyramid 7 wt.%+NW).

As it is seen, the reflection of the surface for the pyramid/nanowire structures is less than nanowires on the silicon surface in the visible spectrum of 300-1000 nm. Additionally, reflection of the formed pyramids in the 3% KOH solution, is less than that of other concentrations. The average reflection of the double-structured surface is approximately 2.5% in the wavelengths of 300-1000 nm. Reflection reduction for this structure is due to the multiple reflections from the textured surface, which helps better entrapment of the incident light in the structure. A schematic of this occurrence is shown in Fig. 8. These structures can be potentially utilized as an anti-reflection textured coating in the solar cells for improving performance and efficiency.

Raman spectroscopy is a kind of interaction between light and matter, which is subjected to nonelastic dispersion in this light spectrometry. In Raman spectroscopy, single-wavelength photons are focused on the sample. Moreover, the laser is usually used as a high-intensity single-light source. The result of the photons' interaction with the molecules of the matter is their

reflection, absorbance, or dispersion. Raman spectroscopy deals with scattered photons. The wavelengths of photons in the Raman dispersion are shifted by the loss or absorption of the energy, so scattered photons are divided into two groups of stokes and anti-stokes. The first group, with the higher wavelength than the original wavelength, is called stokes, and the second group, which has shorter wavelength than the original wavelength, is called anti-stokes.

Figures 9 and 10 present the Raman spectroscopy results of the bare Si, pyramid, and pyramid/nanowire composite structures. The key observation is that all of the samples exhibit a Raman peak at 520 cm^{-1} that is related to the crystalline silicon. This peak represents the stokes spectroscopy. It is worth mentioning that, KOH concentration doesn't affect the position of the peak in the silicon pyramids Raman spectrum. This means that no significant crystal damage has occurred after the etching process [38].

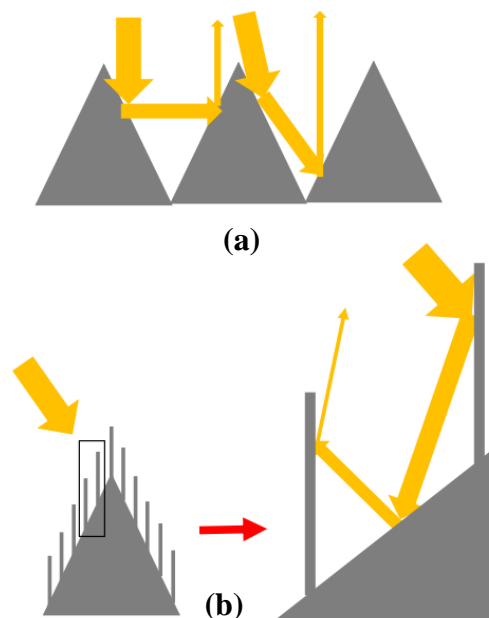


Figure 8. Multiple reflections of incident light from, (a) pyramid and (b) pyramid/nanowire textured substrates.

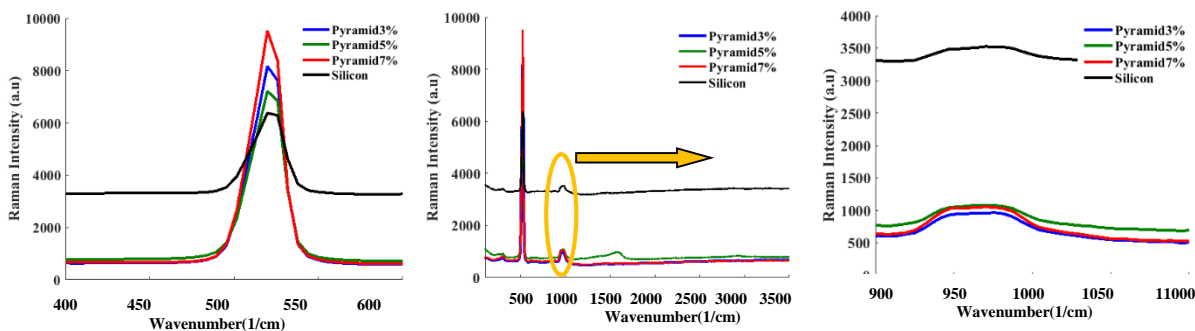


Figure 9. Raman spectra of the bare and pyramidal structured silicon substrates.

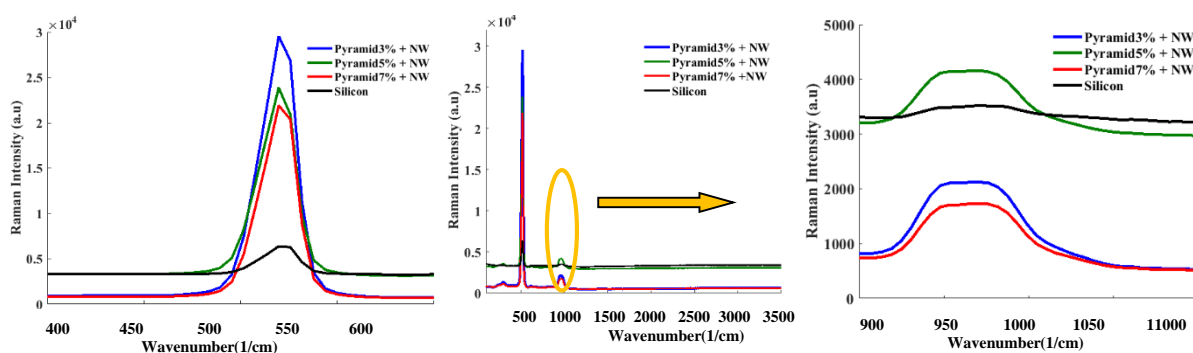


Figure 10. Raman spectra of the bare silicon and pyramid/ nanowire composite structures.

Moreover, the occurred peak at 520 cm^{-1} for the synthesized pyramids on the silicon substrate in different concentrations of the KOH, has the same shape. The peaks of the intensity for the pyramid structures are higher than the simple silicon surface. Furthermore, the absorption rate of these structures is also better. The peaks of the Raman spectrum intensity for the synthesized pyramids in different concentrations of the KOH are different, and the highest peak intensity is related to the synthesized pyramids in the 7 wt.% KOH solution. The second peak at 960 cm^{-1} is related to anti-stokes spectroscopy and has a much lower absorption rate. The intensity of this peak is approximately 10% of the peak at 520 cm^{-1} . However, observations (Fig. 10) show that the peak of the intensity in the Raman spectrum for the binary samples is strongly increased compared to the pyramid-textured samples. However, as can be observed in Fig. 10, the Raman peak intensity at 520 cm^{-1} for the hybrid pyramid structure with the

concentration of 3 wt.% KOH is higher than other hybrid structures. The intensity of the Raman peak for the hybrid structures is approximately 30 times higher than pyramids. Surface morphology and particle size are effective parameters in increasing Raman peak intensity [39].

Figure 11 shows the X-Ray Diffraction (XRD) analysis for the synthesized pyramids in the 3% KOH solution and the composite structure of these pyramids with the nanowires. This spectrometry is performed through the Xpert High score software. The main peak of the spectrum in the mentioned structures occurs at the angle of $2\theta=69.3825^\circ$, which is related to the (400) Si-cubic structure (JCPDS Card No.01-027-1402).

The FWHM for the synthesized pyramids in the 3 wt.% KOH solution and the composite structure is 2.4 and 1.2, respectively, which indicates higher porosity for the composite structures.

A comparison of this work with other similar works is summarized in table 1. As

it is obvious, the average and minimum reflection in this work are smaller than other similar publications, which can be attributed to the uniform distribution of the combined textures of the silicon substrate,

thanks to the pre-treatment process using silver-assisted MACE process, which makes them porous and improves the formation of the later micro pyramids.

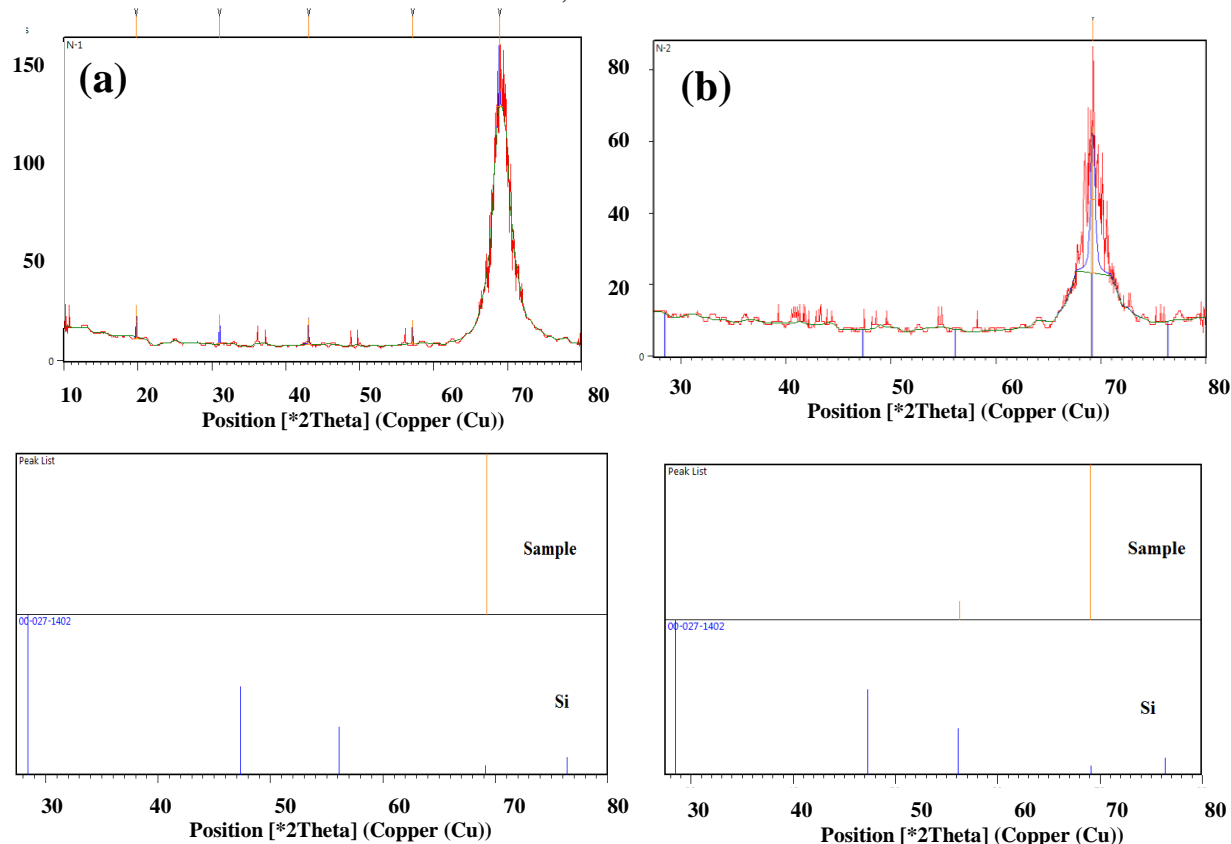


Figure 11. X-ray diffraction pattern for the (a) pyramidal structures and (b) pyramid/nanowire composite structure (pyramids are formed in the 3 wt.% of KOH solution).

Table 1. Comparison table for the several combinatorial structures pyramid/ nanowires.

| Reference | Structure | Textured method | Meta l | Min reflection % | Avg reflection % | Wavelength range |
|------------------|------------------|-----------------|--------|------------------|------------------|------------------|
| [7] | Pyramid/nanowire | MACE | Ag | <3 | <5 | 300-1100 |
| [27] | Pyramid/nanowire | MACE | Ag | 1.1 | 2.4 | 300-2000 |
| [33] | Pyramid/nanowire | MACE | Ag | 2 | <6 | 200-1000 |
| [34] | Pyramid/nanowire | MACE | Ag | <2 | <3 | 200-1000 |
| [35] | Pyramid/nanowire | MACE | Ag | <0.2 | <7 | 400-1000 |
| <i>This work</i> | Pyramid/nanowire | MACE | Ag | 0.1 | <3 | 300-1000 |

4. CONCLUSION

In this work, enhanced anti-reflective properties are achieved using double texturization of the silicon substrate. For this purpose, silicon nanowires were applied to the synthesized pyramidal textures of the silicon wafer. To realize the Si pyramids, an alcoholic solution containing KOH and IPA with different concentrations of 3, 5, and 7 wt.% was employed. Decreasing KOH solution concentration tended to the formation of smaller pyramids which declined reflectivity for the formed pyramids. Meanwhile, the uniformity of the structures

in the concentration of 3 wt.% for KOH solution was better than other concentrations. Adding nanowires to the formed pyramids was performed using silver-assisted chemical etching of the silicon. The combined nanowire/pyramid structures significantly reduced the surface reflection to 2.5% over a broad range in the visible spectrum. X-ray diffraction (XRD) results confirmed Si-cubic structures of the textured substrate. The reduced reflection of the pyramid/nanowire texture makes it suitable for application as tissue coatings in solar cells.

REFERENCES

1. Amri, C., Ouertani, R., Hamdi, A., Ezzaouia, H., "Effect of Silver-Assisted Chemical Vapor Etching on morphological properties and silicon solar cell performance", *Materials Science in Semiconductor Processing*, 63 (2017) 176-183.
2. Liu, Y., Zi, W., Liu, S. F., Yan, B., "Effective light trapping by hybrid nanostructure for crystalline silicon solar cells", *Solar Energy Materials and Solar Cells*, 140 (2015) 180-186.
3. Fang, H., Li, X., Song, S., Xu, Y., Zhu, J., "Fabrication of slantingly-aligned silicon nanowire arrays for solar cell applications", *Nanotechnology*, 19 (2008) 255703.
4. Imahori, H., Umeyama, T, Ito, S., "Large p-aromatic molecules as potential sensitizers for highly efficient dye-sensitized solar cells", *Accounts of chemical research*, 42 (2009) 1809-1818.
5. Velez, V. H., Sundaram, K. B., "Area Effect of Reflectance in Silicon Nanowires Grown by Electroless Etching", *International Journal of Nanoscience and Nanotechnology*, 13 (2017) 283-288.
6. Nishijima, Y., Komatsu, R., Ota, S., Seniutinas, G., Balčytis, A., Juodkazis, S., "Anti-reflective surfaces: Cascading nano/microstructuring", *APL Photonics*, 1 (2016) 076104.
7. Zhang, Z. L., Wang, B., Chen, Y., Tang, Y. H., Song, X. M., Li, Q. L., Yan, H., "Preparation of pyramid-SiNWs binary structure with Ag nanoparticles-assisted chemical etching", *Rare Metals*, (2015) 1-4.
8. Sreejith, K. P., Sharma, A. K., Basu, P.K., Kottantharayil, A., "Etching methods for texturing industrial multi-crystalline silicon wafers: A comprehensive review", *Solar Energy Materials and Solar Cells*, 238 (2022) 111531.
9. Balzereit, S., Proes, F., Altstädt, V., Emmelmann, C., "Properties of copper modified polyamide 12-powders and their potential for the use as laser direct structurable electronic circuit carriers", *Additive Manufacturing*, 23 (2018) 347-354.
10. Spancken, D., van der Straeten, K., Beck, J., Stötzner, N., "Laser Structuring of Metal Surfaces for Hybrid Joints", *Lightweight Design worldwide*, 11 (2018) 16-21.
11. Wang, Q., Zhou, W., "Direct fabrication of cone array microstructure on monocrystalline silicon surface by femtosecond laser texturing", *Optical Materials*, 72 (2017) 508-512.
12. Khadtare, S., Bansode, A. S., Mathe, V. L., Shrestha, N. K., Bathula, C., Han, S. H., Pathan, H. M., "Effect of oxygen plasma treatment on performance of ZnO based dye sensitized solar cells", *Journal of Alloys and Compounds*, 724 (2017) 348-352.
13. Sheikhshoei, F., Mehran, M., Sheikhshoei, I., "Effect of Nano-Textured Silicon Substrate on the Synthesize of Metal Oxides Nanostructures ", *International Journal of Nanoscience and Nanotechnology*, 13 (2017) 265-274.
14. Omar, K., Salman, K. A., "Effects of Electrochemical Etching Time on the Performance of Porous Silicon Solar Cells on Crystalline n-Type (100) and (111)", *Journal of Nano Research*, 46. Trans Tech Publications, (2017) 45-56.
15. Salman, K. A., "Effect of surface texturing processes on the performance of crystalline silicon solar cell", *Solar Energy*, 147 (2017) 228-231.
16. Yoo, C. Y., Meemongkolkiat, V., Hong, K., Kim, J., Lee, E., Kim, D. S., "Reactive Ion Etching Process Integration on Monocrystalline Silicon Solar Cell for Industrial Production", *Current Photovoltaic Research*, 5.4 (2017) 105-108.

17. Zin, N., "Recombination-free reactive ion etch for high efficiency silicon solar cells", *Solar Energy Materials and Solar Cells*, 172 (2017) 55-58.
18. Kulesza-Matlak, G., Gawlińska, K., Starowicz, Z., Sypień, A., Drabczyk, K., Drabczyk, B., Lipiński, M., Zięba, P., "Black Silicon Obtained in Two-Step Short Wet Etching as a Texture for Silicon Solar Cells—Surface Microstructure and Optical Properties Studies", *Archives of Metallurgy and Materials*, 63 (2018).
19. Salhi, B., Hossain, M. K., Al-Sulaiman, F., "Wet-chemically etched silicon nanowire: Effect of etching parameters on the morphology and optical characterizations", *Solar Energy*, 161 (2018.) 180-186.
20. Yang, C. R., Chen, P. Y., Yang, C. H., Chiou, Y. C., Lee, R. T., "Effects of various ion-typed surfactants on silicon anisotropic etching properties in KOH and TMAH solutions", *Sensors and Actuators A: Physical*, 119 (2005) 271-281.
21. Fellahi, O., Hadjersi, T., Maamache, M., Bouanik, S., Manseri, A., Guerbous, L., "Influence of crystalline damage on morphological and optical properties of silicon nanowires", *Optical Materials*, 32 (2010) 768-771.
22. Zubeł, I., Kramkowska, M., "The effect of isopropyl alcohol on etching rate and roughness of (1 0 0) Si surface etched in KOH and TMAH solutions", *Sensors and Actuators A: Physical*, 93.2 (2001) 138-147.
23. Silva, A. R., Miyoshi, J., Diniz, J. A., Doi, I., Godoy, J., "The surface texturing of monocrystalline silicon with NH₄OH and ion implantation for applications in solar cells compatible with CMOS technology", *Energy Procedia*, 44 (2014) 132-137.
24. Chen, Y., Zhang, C., Li, L., Tuan, C. C., Wu, F., Chen, X., Gao, J., Ding, Y., Wong, C. P., "Fabricating and controlling silicon zigzag nanowires by diffusion-controlled metal-assisted chemical etching method", *Nano letters*, 17 (2017) 4304-4310.
25. Chen, Y., Li, L., Zhang, C., Tuan, C. C., Chen, X., Gao, J., Wong, C. P., "Controlling kink geometry in nanowires fabricated by alternating metal-assisted chemical etching", *Nano letters*, 17.2 (2017) 1014-1019.
26. Leon, J. J. D., Hiszpanski, A. M., Bond, T. C., Kuntz, J. D., "Design Rules for Tailoring Antireflection Properties of Hierarchical Optical Structures", *Advanced Optical Materials*, 5 (2017) 1700080.
27. Pei, Z., Hu, H., Li, S., Ye, C., "Fabrication of Orientation-Tunable Si Nanowires on Silicon Pyramids with Omnidirectional Light Absorption", *Langmuir*, 33 (2017) 3569-3575.
28. Martín-Palma, R. J., Vazquez, L., Herrero, P., Martínez-Duart, J. M., Schnell, M., Schaefer, S., "Morphological, optical and electrical characterization of anti-reflective porous silicon coatings for solar cells", *Optical Materials*, 17 (2001) 75-78.
29. Li, Q., Gao, J., Li, Z., Yang, H., Liu, H., Wang, X., Li, Y., "Absorption enhancement in nanostructured silicon fabricated by self-assembled nanosphere lithography", *Optical Materials*, 70 (2017) 165-170.
30. Rahman, T., Boden, S. A., "Optical modeling of black silicon for solar cells using effective index techniques", *IEEE Journal of Photovoltaics*, 7 (2017) 1556-1562.
31. Li, J. Y., Hung, C. H., Chen, C. Y., "Hybrid black silicon solar cells textured with the interplay of copper-induced galvanic displacement", *Scientific reports*, 7 (2017) 17177.
32. Chen, H. Y., Lu, H. L., Ren, Q. H., Zhang, Y., Yang, X. F., Ding, S. J., Zhang, D. W., "Enhanced photovoltaic performance of inverted pyramid-based nanostructured black-silicon solar cells passivated by an atomic-layer-deposited Al₂O₃ layer", *Nanoscale*, 7 (2015) 15142-15148.
33. Song, Y., Kim, K., Choi, K., Ki, B., Oh, J., "Nano/micro double texturing of antireflective subwavelength structures on inverted pyramids", *Solar Energy*, 135 (2016) 291-296.
34. Singh, P., Srivastava, S. K., Yameen, M., Sivaiah, B., Prajapati, V., Prathap, P., Laxmi, S., Singh, B. P., Rauthan, C. M. S., Singh, P. K., "Fabrication of vertical silicon nanowire arrays on three-dimensional micro-pyramid-based silicon substrate", *Journal of materials science*, 50 (2015) 6631-6641.
35. Pant, N., Singh, P., Srivastava, S. K., Shukla, V. K., "Fabrication of nanowire arrays over micropyramids for efficient Si solar cell", *AIP Conference Proceedings*, 1728 (2016) 020451.
36. Rahman, T., Navarro-Cía, M., Fobelets, K., "High density micro-pyramids with silicon nanowire array for photovoltaic applications", *Nanotechnology*, 25 (2014) 485202.
37. Peng, K. Q., Hu, J. J., Yan, Y. J., Wu, Y., Fang, H., Xu, Y., Lee, S., Zhu, J., "Fabrication of Single-Crystalline Silicon Nanowires by Scratching a Silicon Surface with Catalytic Metal Particles", *Advanced Functional Materials*, 16 (2006) 387-394.
38. Singh, P., Srivastava, S. K., Yameen, M., Sivaiah, B., Prajapati, V., Prathap, P., Laxmi, S., Singh, B. P., Rauthan, C. M. S., Singh, P. K., "Fabrication of vertical silicon nanowire arrays on three-dimensional micro-pyramid-based silicon substrate" *Journal of Materials Science*, 50 (2015) 6631-6641.
39. Liu, F. M., Ren, B., Wu, J. H., Yan, J. W., Xue, X. F., Mao, B. W., Tian, Z. Q., "Enhanced-Raman scattering from silicon nanoparticle substrates", *Chemical physics letters*, 382.5-6 (2003) 502-507.